

## Quantum diffusion of muonium in the alkali halides

T. McMullen and J. Meng\*

*Department of Physics, Virginia Commonwealth University, Richmond, Virginia 23284-2000*

J. M. Vail

*Department of Physics, University of Manitoba Winnipeg, Manitoba, Canada R3T 2N2*

P. Jena

*Department of Physics, Virginia Commonwealth University, Richmond, Virginia 23284-2000*

(Received 21 February 1995)

Electronic-structure calculations are described for muonium in NaF, giving a value for the transfer-matrix element  $|t^{(0)}| \simeq 9$  mK and a muonium-phonon coupling strength characterized by a deformation potential  $|E_d| \simeq 2.6$  eV. When used in the small polaronic quantum diffusion model, these values do give the crossover from coherent to incoherent tunneling at  $\sim 100$  K, as observed in other alkali halides. However, a large upward renormalization of  $|t^{(0)}|$  is needed if this theory is to give the observed tunneling rates.

### I. INTRODUCTION

Studies of the motion of muonium (Mu) in insulating crystals provide a fundamental test of our ideas of quantum motion of light impurities in solids. A minimum is observed in the relaxation rate of the muons of muonium (Mu) as a function of temperature in alkali halide and other insulating crystals. In the alkali halides, this minimum occurs at  $\simeq 70$  K in KCl (Ref. 1) and  $\simeq 50$  K in NaCl<sup>2</sup>, and is interpreted as the crossover from coherent to incoherent quantum diffusion. By 20 K in NaCl, Mu appears to be delocalized in a coherent wave function spanning several sites.<sup>2</sup> In solid N<sub>2</sub>, a minimum in the Mu inverse residence time on a site is seen at  $\simeq 50$  K, along with other interesting behavior.<sup>3</sup> One of the Mu species in CuCl shows a similar minimum.<sup>4</sup> Because the crystals are insulating, these studies provide the first experimental examples of quantum diffusion around the coherent-incoherent crossover that are uncontaminated by the effects of conduction electrons.

Theories of quantum motion of light impurities in solids (Sec. VI) basically begin with the small polaron model<sup>5-8</sup> of a particle which tunnels between adjacent lattice sites and is linearly coupled to phonons through a site-diagonal interaction,

$$H = -t \sum_{\langle lm \rangle} c_l^\dagger c_m + \text{H.c.} + \sum_{\mathbf{q}\lambda} \omega_{\mathbf{q}\lambda} a_{\mathbf{q}\lambda}^\dagger a_{\mathbf{q}\lambda} + \sum_{l\mathbf{q}\lambda} g_{l\mathbf{q}\lambda} c_l^\dagger c_l \phi_{\mathbf{q}\lambda}, \quad (1)$$

where  $c_l^\dagger$  creates an electron on site  $l$ ,  $a_{\mathbf{q}\lambda}^\dagger$  creates a phonon of wave vector  $\mathbf{q}$  and polarization  $\lambda$ , and  $\phi_{\mathbf{q}\lambda} = a_{\mathbf{q}\lambda} + a_{-\mathbf{q}\lambda}^\dagger$ . The small polaronic theory of the crossover from coherent to incoherent quantum diffusion<sup>5-7</sup> gives a minimum in the tunneling rate at the temperature where

the impeding of coherent bandlike propagation by increasing numbers of thermal phonons is short circuited by the decrease in the effective barrier height that accompanies increased thermal vibration. However, the (partly) renormalized tunneling matrix element  $t$  and phonon coupling  $g_{l\mathbf{q}\lambda}$  appearing in the small polaron Hamiltonian (1) are not<sup>8</sup> the bare  $t^{(0)}$  and  $g_{l\mathbf{q}\lambda}^{(0)}$  that would result from a microscopic calculation based on the actual Mu potential energy surface within the rigid host crystal. Instead, Shore and Sander<sup>9</sup> found that  $t$  as deduced from experiments on impurities in alkali halides was appreciably larger (by factors of  $10^2 - 10^6$ ) than reasonable estimates of the microscopic  $t^{(0)}$ . The reasons for this are becoming clear.<sup>8,10-12</sup> The state space of the particle has been truncated<sup>10</sup> in (1) to the Wannier states of the lowest band, so the particle's dynamics during tunneling are lost. In reality, the high-frequency modes of the environment follow the particle nearly adiabatically, reducing the effective barrier heights. Since this dynamical effect has been lost, it must be incorporated in  $t$ . Although a general framework for the calculation of this renormalization  $t^{(0)} \rightarrow t$  is now in place,<sup>8,10-12</sup> no estimates of its magnitude are yet available. This is partly because values of the microscopic  $t^{(0)}$  have not been available for comparison. Additional information about the Mu potential in the distorted lattice will also be needed to make quantitative comparison of the theories with experiment.

This information about the potential surfaces and particle-phonon interactions will come from electronic-structure calculations giving the energy of the impurity as a function of lattice configuration. We demonstrate here that such calculations are practical for Mu in an alkali halide. We report our estimates of the microscopic intersite transfer-matrix elements  $t^{(0)}$  and particle-phonon coupling strengths  $g_{l\mathbf{q}\lambda}^{(0)}$  for Mu in an alkali halide in Secs. III and IV, respectively. These are the two basic parameters needed to begin a quantitative comparison

of theory and experiment. Our estimates use the standard methods<sup>13,14</sup> of electronic-structure calculation for defects in insulators. With further work, it should be possible to obtain more information about the potential energy surfaces to make comparisons of theory with experiment beyond this initial and elementary attempt. On the assumption that Mu will behave similarly in all the alkali halides, we chose NaF because it is relatively easy to simulate.

However, an important observation results from the present work. We find that using our microscopic values in place of  $t$  and  $g_{lq\lambda}$  in the truncated Hamiltonian (1) does give a crossover temperature  $T_{\text{coh}} \sim 100$  K in this material, as observed in the other alkali halides. On the other hand, the calculated residence time is orders-of-magnitude longer than that observed. This implies an upward renormalization  $t/t^{(0)} \sim 10^2$ . This large value is surprising, given the characteristic zero-point frequency  $\omega_{\text{cl}} \simeq 4900$  K that we find for this very light impurity, which is far higher than any of the phonon frequencies of the host crystal.

## II. MUONIUM POTENTIAL

The energy of Mu in NaF was calculated for various  $\mu^+$  positions using the ICECAP methodology<sup>13,14</sup> for point defects in ionic crystals. The total energy of the system is evaluated for given positions of the impurity nucleus (here a positive muon,  $\mu^+$ ) and of the host ion nuclei. The electrons of the neighboring ions, and the Mu electron, are treated fully quantum mechanically as an all-electron molecular cluster using the unrestricted Hartree-Fock self-consistent field approximation. The rest of the crystal is described by classical shell-model ions in equilibrium with the quantum cluster.<sup>15</sup>

$\text{Na}^+$  and  $\text{F}^-$  are isoelectronic, and since Mu is neutral the two different ions are almost indistinguishable to it. Consequently, the lattice seen by the Mu is simple cubic, with the classical Mu sites at the centers of cubes of side  $d$  having four ions of each kind at the corners.<sup>16</sup> The Mu potential was found by moving the  $\mu^+$  around

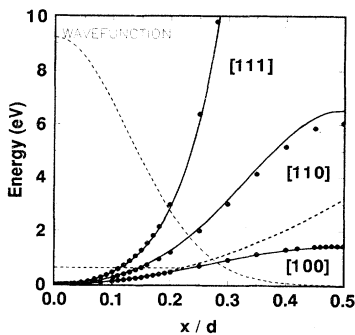


FIG. 1. Muonium potential in three directions from the interstitial site. The solid curves are the fit described in the text. The dashed curves show our best isotropic parabola fit near the minimum, and (as lighter lines) the corresponding energy ( $3\hbar\omega_{\text{cl}}/2$ ) and wave function.

within this cube, using as the quantum cluster two adjoining cubes (12 ions). Since the computer time needed to compute the energy for a single  $\mu^+$  position is significant and since the Mu band is expected to be narrow, the full Mu potential surface was not mapped out. Instead, the energy in the rigid lattice with  $d = 2.31$  Å (the equilibrium spacing) was calculated for  $\mu^+$  positions along various symmetry directions in the fundamental  $1/32$  of the cube (Fig. 1).

In addition, the relaxation energy was evaluated when the ions of the quantum cluster and the rest of the crystal relax to equilibrium with the Mu in its activated (saddle-point) position at the center of the common face between the two cubes.

## III. TUNNELING MATRIX ELEMENT

### A. Numerical calculation

The results of our calculations of the Mu potential in the rigid lattice (with  $d = 2.31$  Å) were reasonably well described by a potential of  $(135 \text{ eV}) \times \exp(-[6|\mathbf{r} - \mathbf{R}_{\text{ion}}|/d]^{1.15})$  placed at each ion site. The resulting potential is shown as solid curves in Fig. 1, and was used to interpolate the calculated potential throughout the crystal. The Schrodinger equation for a  $\mu^+$  in this potential was then solved by a numerical relaxation technique<sup>17</sup> for two boundary conditions on the cube faces, odd ( $\mathbf{k} = \pi, \pi, \pi$ ) and even ( $\mathbf{k} = 0$ ) parity. The difference of the two energies gives the rigid-lattice bandwidth,  $W = 12|t^{(0)}|$ . The results of calculations for different numbers of mesh points within  $1/8$  of the cube of side  $d$  are given in Table I. Although changing the mesh spacing shifts the band by much more than the very narrow bandwidth, the width remains consistently  $\sim 10 \mu\text{eV}$ , leading to our estimate of the bare tunneling matrix element  $t^{(0)} \sim -9$  mK.

TABLE I. Bandwidths calculated numerically using various mesh spacings. An  $N \times N \times N$  mesh has  $N - 1$  equal divisions along each direction within  $1/8$  of the simple cubic unit cell. The bottom of the band is at  $\mathbf{k} = 0$ , and the top of the band is at  $\mathbf{k} = (\pi, \pi, \pi)$ . The transfer-matrix element is given by  $t = -W/12$ , where  $W$  is the bandwidth. The result of the approximate (tight-binding) calculation and the energy as estimated by the zero-point energy in the parabolic well fitted around the  $\mu^+$  site are given in the last row.

Mesh	$E_{\mathbf{k}=(\pi,\pi,\pi)}$ (eV)	$E_{\mathbf{k}=0}$ (eV)	$W$ ( $\mu\text{eV}$ )	$t$ (mK)
$21 \times 21 \times 21$	0.657 751	0.657 741	10.1	-9.7
$31 \times 31 \times 31$	0.658 753	0.658 744	9.57	-9.3
$41 \times 41 \times 41$	0.659 103	0.659 094	9.41	-9.1
$51 \times 51 \times 51$	0.659 265	0.659 256	9.33	-9.1
Approximate	0.629		4.9	-4.8

### B. Approximate calculation

In addition, the tight-binding method as described by Ashcroft and Mermin<sup>18</sup> was used to estimate  $t^{(0)}$ . To do so, only potential in the regions in the vicinity of the minimum at the cube center and around the saddle point at the face center were needed. Around the cube center, an isotropic harmonic potential is a good approximation, shown as the dashed line in Fig. 1. This harmonic potential was used as the “atomic” potential of the tight-binding method, and the corresponding well-localized oscillator wave function is also shown. The two-center integrals involve the overlap of these wave functions on adjacent sites, which is only significant near the face-center saddle point, and were evaluated using a quadratic fit to the potential in that region. The result of this estimate is  $t^{(0)} \sim -5$  mK, in satisfactory agreement with the numerical calculations.

### IV. DEFORMATION POTENTIAL PARAMETER

Mu is a neutral particle, and as such sees little difference between the positive and negative ions and experiences only short-range forces exerted by the ions. Thus, the predominant Mu-phonon coupling is to the longitudinal-acoustic phonon branch, and the strength of this coupling can be characterized by a deformation potential  $E_d$ . This was evaluated from the force exerted on the  $\mu^+$  by the neighboring ions, given by computations involving small displacements of those ions, with the result  $E_d = -2.64$  eV. For this calculation, the  $\mu^+$  was located at the cube center, a reasonable approximation since the wave function of Fig. 1 is well localized.

### V. RELAXATION ENERGY

The Mu potential in the rigid lattice shown in Fig. 1 is for the situation where the lattice is held rigid and the nuclei do not move at all in response to the motion of the impurity. This is the usual Condon approximation. The opposite extreme would occur if the lattice were to follow the Mu’s motion adiabatically, remaining in equilibrium with it at each position throughout its trajectory. How different are the two cases? From Fig. 1, the barrier height is approximately 1.45 eV for motion from one cube center to an adjacent one. We have evaluated the relaxation energy with the Mu in the saddle-point position at the center of the common face between two cubes. This was done using a quantum cluster consisting of the saddle-point Mu and its four nearest-neighbor ions, which are two  $\text{Na}^+$ ’s and two  $\text{F}^-$ ’s. The relaxation energy to equilibrium is found to be 1.34 eV. This means that the barrier height is reduced from 1.45 to 0.11 eV, i.e., by an order of magnitude. The calculated outward relaxation is substantial but reasonable: the two  $\text{Na}^+$ ’s are radially displaced by 18%, the two  $\text{F}^-$ ’s by 20%, with some associated expansion of the Mu electron’s mean radius. In this calculation *all* ions of the infinite crystal are relaxed to equilibrium. The magnitude of the bar-

rier height reduction in this case supports the view that the renormalization effect  $t^{(0)} \rightarrow t$  could be potentially significant, since it depends roughly exponentially on the barrier height. The question to which we do not yet have an answer is to what extent the barrier has time to respond to the tunneling Mu. The characteristic frequency  $\omega_{cl} \simeq 4900$  K that we find using the rigid-lattice potential of Fig. 1 suggests not very much. The way in which theories of quantum diffusion have begun to address this question in a way which should be calculable by electronic-structure techniques such as those we use here are outlined in Sec. VIC below.

## VI. RELATION TO THEORIES OF QUANTUM DIFFUSION

Quantum propagation is a fascinating subject that spans several regimes and diverse systems.<sup>5,6,8</sup> Both coherent, or bandlike, quasiparticle propagation and incoherent tunneling are possible. Scattering by the environment impedes coherent propagation but assists incoherent motion, so the coherent mobility decreases with increasing temperature while the incoherent mobility increases. Several theories have been discussed in the context of, or seem relevant to, the quantum propagation of Mu, and we summarize them here and discuss the future of calculations using our electronic-structure techniques.

There is a fundamental difference between measurements of muon-spin relaxation ( $\mu\text{SR}$ ) and macroscopic transport measurements.<sup>1,2,19,20</sup>  $\mu\text{SR}$  basically measures the correlation time of the effective magnetic fields at the position of the muon. When these are static fields originating from the surrounding nuclei, their correlation length is about a lattice spacing, and the relevant correlation time is the time-of-stay  $\tau_s$  on a site. In the coherent quantum diffusion regime,  $\tau_s$  is not directly related to the long-range diffusion constant. For example, in small polaron theory the diffusion constant has the well-known  $T^{-9}$  caused by two-phonon scattering in a narrow band.<sup>7</sup> However, since the two-phonon mean free path must remain larger than the lattice spacing for this picture to be valid,  $\tau_s$  is not governed by this scattering and has a different temperature dependence.

### A. Small polaron theory

In the small polaron theory of the truncated Hamiltonian (1) the time-of-stay is<sup>6,7,21</sup>

$$\tau_s^{-1} = \begin{cases} n|t|^2 B^{\text{incoh}}/\hbar^2, & \text{incoherent channel} \\ 2\sqrt{n}|t|^2 Z/\pi\hbar^2, & \text{coherent channel,} \end{cases} \quad (2)$$

where  $n$  is the coordination number and

$$Z = \exp \left\{ - \int_0^\infty \frac{d\omega}{\omega} G(\omega) \coth \left( \frac{\beta\omega}{2} \right) \right\} \quad (3)$$

is a renormalization constant, while

$$B^{\text{incoh}} = Z \int_{-\infty}^{\infty} d\xi \left[ \exp \left\{ \int_0^{\infty} \frac{d\omega}{\omega} \right. \right. \\ \left. \left. \times G(\omega) \frac{\cos(\omega\xi)}{\sinh\left(\frac{\beta\omega}{2}\right)} \right\} - 1 \right]. \quad (4)$$

For the effective phonon density of states  $G$ , which includes the particle-phonon coupling, we use a refinement of an earlier version<sup>21</sup> that is suitable for the alkali-halide structure. The sum over ions appearing in  $g_{i\mathbf{q}\lambda}^{(0)}$  is replaced by a spherical average. Then, using the Debye model and the long-wavelength limit of the coupling function, we obtain

$$G(\omega) = g_0 \omega^2 \left[ \frac{3j_1(z)}{z} \right]^2 \left[ 1 - \frac{\sin x}{x} \right], \quad (5)$$

where  $x = (3\pi^2)^{1/3}\omega$ ,  $z = \sqrt{3}x/2$ , and  $j_1$  is a Bessel function. The coupling constant  $g_0$  is given by

$$g_0 = \frac{3E_d^2}{(\bar{M}s^2)(k_B\Theta_D)} \quad (6)$$

with  $\bar{M}$  the mean ion mass and  $\Theta_D$  the Debye temperature.<sup>22</sup> Our value for  $E_d$  yields  $g_0 = 260$  for Mu in NaF.

The result of using our values of  $t^{(0)}$  and  $E_d$  (or  $g_{i\mathbf{q}\lambda}^{(0)}$ ) in place of  $t$  and  $g_{i\mathbf{q}\lambda}$  to calculate the inverse time-of-stay using Eqs. (2) and (5) is shown as the lower curve in Fig. 2. The crossover temperature is  $T_{\text{coh}} \simeq 140$  K, which is of the same order as observed in KCl (Ref. 1) and NaCl.<sup>2</sup> However, many orders of magnitude separate the observed and calculated rates. To find the renormalized values that would be needed to represent the data, we attempted to fit the KCl data, and show the best overall representation that we found as the upper curve in Fig. 2. The fitted deformation potential  $|E_d| = 1.4$  eV is slightly smaller than that calculated for NaF. The slopes in the incoherent regime and in the coherent regime near

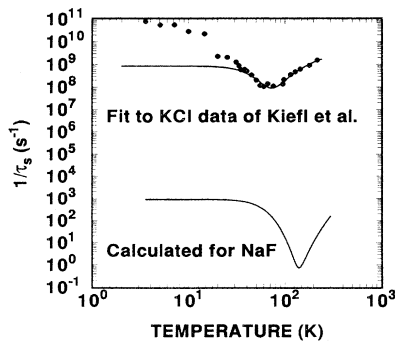


FIG. 2. Inverse time of stay for Mu in alkali halides as a function of temperature, as given by small-polaron theory. The lower curve is for NaF, using our calculated bare values ( $|t^{(0)}| = 9$  mK,  $g_0 = 260$ ,  $\Theta_D = 354$  K). The upper curve is our fit ( $|t^{(0)}| = 2.5$  K,  $g_0 = 120$ ,  $\Theta_D = 200$  K) to the data (points) of Kiefl *et al.* (Ref. 1) for Mu in KCl.

$T_{\text{coh}}$  adequately represent the data there. However, we were unable to reproduce the three orders of magnitude increase in  $1/\tau_s$  that occurs below  $T_{\text{coh}}$ , while keeping  $\Theta_D$  reasonable. Stamp and Zhang<sup>23</sup> have proposed an intriguing alternative, in which  $|t^{\text{eff}}| \equiv \sqrt{Z}|t| \sim 10$  K and an activation energy  $E_a \simeq 33$  meV would fit the data. This activation energy corresponds to  $g_0 \simeq 88$ , which gives  $Z \sim 10^{-5}$ . It is not clear that the rate they consider is related to the correlation time of the effective fields measured in the experiment.

## B. Two-phonon coupling

Quite good fits to the experimental data for Mu relaxation<sup>3</sup> have been found using adjustable parameters in modifications of the small polaron model.<sup>24</sup> One modification that has been included is the effect of two-phonon scattering within the narrow coherent band.<sup>7</sup> This does limit the diffusion constant, but since the two-phonon mean free path should be larger than the lattice spacing for this picture to remain valid, it seems irrelevant to the Mu relaxation rate. A second modification is to attempt to model the barrier fluctuations that lead to level coincidences favorable to tunneling<sup>5</sup> by expanding the transfer matrix element in displacements from the undistorted configuration<sup>25</sup>

$$t(\{\mathbf{R}_i\}) = t^{(0)} + \sum_{\mathbf{q}\lambda} t_{\mathbf{q}\lambda}^{(1)} \phi_{\mathbf{q}\lambda} \\ + \sum_{\substack{\mathbf{q}_1 \lambda_1 \\ \mathbf{q}_2 \lambda_2}} t_{\mathbf{q}_1 \lambda_1 \mathbf{q}_2 \lambda_2}^{(2)} \phi_{\mathbf{q}_1 \lambda_1} \phi_{\mathbf{q}_2 \lambda_2} + \dots \quad (7)$$

The coefficients  $t^{(i)}$  can, in principle, be determined by electronic-structure methods, but the concern is that in situations where these barrier fluctuations are important the effects are too large to be treated by this kind of perturbative expansion. Specifically, the present work (Sec. V) indicates that  $t(\{\mathbf{R}_i\}) \gg t^{(0)}$  for typical  $\mathbf{R}_i$ . An expansion of  $\ln t(\{\mathbf{R}_i\})$  about its minimum to introduce lattice-dynamical effects has been suggested by Kagan and Klinger.<sup>25</sup> The path-integral approach introduces similar effects. The magnitude of the contribution of these phonon effects is not yet known. The relaxation energy calculation of Sec. V shows that, between the cases of no following and instantaneous following of the Mu by the surrounding ions (where the phonon processes would play a role), there is one full order of magnitude in energy. The outstanding question then is, how can these phonon effects be calculated and, when they are, how can they account for the large discrepancy between our rigid-lattice calculation and experiment, in view of the high zero-point frequency of the muon in the crystal compared to the host ion vibration frequencies.

## C. Path integrals

The alternative approach<sup>8,10–12,26</sup> that uses path-integral methods seems to be better suited to these situ-

ations. The approach is based on a saddle-point approximation in which the Euclidean effective action<sup>10,11</sup> (or the influence functional<sup>8,26</sup>) for the tunneling particle is expanded about a “classical trajectory” that minimizes this effective action. To find this instanton trajectory through realistic computations, the particle-lattice interactions and phonon modes are needed. Sections II–IV show how the former can be computed. Likely the harmonic approximation will be used initially, and it is not yet known how important the effects of lattice anharmonicity may be.

The saddle-point approximation suggests that there is a characteristic time interval during which the lattice can respond to the particle as it tunnels. The instanton path, which is the classical Euclidean trajectory in the effective potential, identifies this interval as the duration of the “flip” where the tunneling particle crosses from one site to the next.<sup>10,11</sup> The only phonon modes that can follow the particle adiabatically as it tunnels are those with frequencies that are high on the scale of this flip time. Mu is an extremely light impurity, and the characteristic classical frequency  $\omega_{cl}$  that we calculate in NaF (4900 K) is far higher than any phonon frequencies. If the frequencies characterizing the instanton trajectory are  $\sim \omega_{cl}$ , the high-frequency renormalization  $t^{(0)} \rightarrow t$  should be small. Such large renormalization would, instead, seem to require the characteristic frequencies to be smaller than  $\Theta_D$ . If this were true, the resulting temperature dependence could be related to the inability of small polaron theory to reproduce the large change with temperature below  $T_{coh}$ . Our fitted  $|t|$  for KCl is 300 times larger than our calculated  $|t^{(0)}|$  for NaF. This is similar to the

differences found by Shore and Sander.<sup>9–11</sup> However, the circumstances are somewhat different.

## VII. SUMMARY

In summary, we have estimated the bare or microscopic transfer-matrix element  $t^{(0)}$  and particle-phonon coupling strength  $E_d$  for Mu in an alkali halide. Comparison of our result for  $t^{(0)}$  with the experimental data shows that a large upward renormalization must occur on transforming to the usual (truncated) small polaron model Hamiltonian of quantum diffusion. We have also estimated the strength of the Mu-phonon coupling. The values of these two fundamental parameters uncover puzzling aspects of quantum tunneling as observed by elegant  $\mu$ SR experiments. We hope that this provides impetus toward a quantitative theory, possibly based on the existing path-integral formulations.

## ACKNOWLEDGMENTS

We thank Z. Yang for performing some of the calculations leading to  $E_d$ . This work was supported by the Department of Energy under Grant No. DE-FG05-87-ER45316 and by the Natural Sciences and Engineering Research Council of Canada and the Research Board of the University of Manitoba. J.M.V. gratefully acknowledges the hospitality of Virginia Commonwealth University during part of this work.

- 
- \* Present address: General Sciences Corp., Laurel, MD.
- <sup>1</sup> R. F. Kiefl, R. Kadono, J. H. Brewer, G. M. Luke, H. K. Yen, M. Celio, and E. J. Ansaldo, *Phys. Rev. Lett.* **62**, 792 (1989).
  - <sup>2</sup> R. Kadono, R. F. Kiefl, E. J. Ansaldo, J. H. Brewer, M. Celio, S. R. Kreitzman, and G. M. Luke, *Phys. Rev. Lett.* **64**, 665 (1990).
  - <sup>3</sup> V. Storchak, J. H. Brewer, W. N. Hardy, S. R. Kreitzman, and G. D. Morris, *Phys. Rev. Lett.* **72**, 3056 (1994).
  - <sup>4</sup> J. W. Schneider, R. F. Kiefl, K. Chow, S. F. J. Cox, S. A. Dodds, R. C. DuVarney, T. L. Estle, R. Kadono, S. R. Kreitzman, R. L. Lichti, and C. Schwab, *Phys. Rev. Lett.* **68**, 3196 (1992).
  - <sup>5</sup> T. Holstein, *Ann. Phys. (N.Y.)* **8**, 343 (1959).
  - <sup>6</sup> C. P. Flynn and A. M. Stoneham, *Phys. Rev. B* **1**, 3966 (1970).
  - <sup>7</sup> Yu. Kagan and M. I. Klinger, *J. Phys. C* **7**, 2791 (1974).
  - <sup>8</sup> A. J. Leggett, S. Chakravarty, A. T. Dorsey, M. P. A. Fisher, A. Garg, and W. Zwerger, *Rev. Mod. Phys.* **59**, 1 (1987).
  - <sup>9</sup> H. B. Shore and L. M. Sander, *Phys. Rev. B* **12**, 1546 (1976).
  - <sup>10</sup> J. P. Sethna, *Phys. Rev. B* **24**, 698 (1981).
  - <sup>11</sup> J. P. Sethna, *Phys. Rev. B* **25**, 5050 (1982).
  - <sup>12</sup> A. O. Caldeira and A. J. Leggett, *Ann. Phys. (N.Y.)* **149**, 374 (1983).
  - <sup>13</sup> J. H. Harding, A. H. Harker, P. B. Keegstra, R. Pandey, J. M. Vail, and C. Woodward, *Physica* **131B**, 151 (1985).
  - <sup>14</sup> J. M. Vail, *J. Phys. Chem. Solids* **51**, 589 (1990).
  - <sup>15</sup> The intuitively apparent procedure used here has been derived using a theory of the interaction of a quantum impurity with an ionic crystal in the harmonic approximation consistent with the ICECAP methodology by J. M. Vail, T. McMullen, and J. Meng, *Phys. Rev. B* **49**, 193 (1994).
  - <sup>16</sup> A nice experimental demonstration of the inability of a neutral species to distinguish the two kinds of ion is given by the data of J. Kasi and K. Fujiwara, *J. Phys. Soc. Jpn.* **51**, 3077 (1982) on positronium momentum distributions in alkali halides, where the odd-index peaks are almost invisible, as in a simple cubic lattice.
  - <sup>17</sup> G. E. Kimball and G. H. Shortley, *Phys. Rev.* **45**, 815 (1934); M. J. Puska and R. M. Nieminen, *Phys. Rev. B* **29**, 5382 (1984).
  - <sup>18</sup> N. W. Ashcroft and N. D. Mermin, *Solid State Physics* (Saunders College, Philadelphia, 1976).
  - <sup>19</sup> T. McMullen and E. Zaremba, *Phys. Rev. B* **18**, 3026 (1978), give an example of the local nature of depolarizing fields in a different context. They discuss the behavior of the magnetic-field correlation functions for the nuclear dipole fields causing  $\mu^+$  depolarization in a metal.

- <sup>20</sup> T. McMullen, *Solid State Commun.* **35**, 221 (1980).
- <sup>21</sup> T. McMullen and B. Bergersen, *Solid State Commun.* **28**, 31 (1978).
- <sup>22</sup> The appropriate Debye temperatures represent an average of the sound velocity over the entire Brillouin zone. These were approximated by the TO phonon temperatures from Ref. 18, Table 27.2.
- <sup>23</sup> P. C. E. Stamp and C. Zhang, *Phys. Rev. Lett.* **66**, 1902 (1991).
- <sup>24</sup> Yu. Kagan and N. V. Prokofev, *Phys. Lett.* **150**, 320 (1990).
- <sup>25</sup> Yu. Kagan and M. I. Klinger, *Sov. Phys. JETP* **43**, 132 (1976).
- <sup>26</sup> S. Chakravarty and A. J. Leggett, *Phys. Rev. Lett.* **52**, 5 (1984).